IEEE Transactions on Nuclear Science, Vol.NS-22, February 1975

CHARGE CARRIER TRANSPORT PROPERTIES OF SEMICONDUCTOR MATERIALS SUITABLE FOR NUCLEAR RADIATION DETECTORS

G. Ottaviani, C. Canali and A. Alberigi Quaranta
Istituto di Fisica dell'Università, Via Vivaldi 70,
41100 Modena, Italy and
I.N.F.N., Sezione Bologna, Italy

ABSTRACT

Charge carrier drift velocities in semiconductor materials suitable for solid state detectors has been reviewed. Si, Ge, CdTe and GaAs are considered. New data for HgI_2 recently obtained are also reported. The data cover a large range of temperatures (6-430 K) and electric fields up to 50 KV/cm. An anisotropy effect in the drift velocity obtained by applying the electric field parallel to different crystallographic axis is also discussed for the case of Si and Ge.

INTRODUCTION

The use of semiconductor materials for nuclear detectors has required a better knowledge of the physical properties of the materials itself. The first researches were devoted to correlate the numbers of the carriers created in the detector and the energy loss by the impinging nuclear radiation[1-5]. The researches in this field had as main purpose the measurements of the mean energy necessary to produce an electron-hole pair in different materials and correlate such data with the energy gap and with the energy loss by the radiation[6-13]. However the use of detectors for timing in addition to spettrometry has pointed out the necessity to know the transport properties (drift velocity, plasma time ecc.) of the charge carriers produced in the detector by the radiation[1]. Charge carriers transport properties as drift velocity, plasma time ecc. which are related to the timing characteristics of the detectors have been investigated initially for this reason.

Moreover detectors obtained from semiconductor compounds or from Ge and Si compensated material have emphasized the importance of trapping and detrapping effects[1,14-16]. Such effects not only affect the time response of the detector but also the numbers of the carriers collected at the electrodes and consequently the resolution power. It has been shown in fact[1,14-16] that for having a good resolution power it is necessary not only to create a number of carriers as large as possible but also to collect completely them on suitable contacts. An easy correlation between the charge collected at the electrodes and the trapping and detrapping effect is impossible since such correlation depends upon the values of transit, trapping and detrapping time of the carriers. For istance when both the charge carriers have transit time much shorter respect trapping and detrapping time the effect of the latters are negligible[1,16] on the shape of the waveform supplied by the detector; while in the case of comparable times the above quoted correlation is very difficult[1,16]. Moreover the charge carriers transport properties strongly dependent upon temperature, electric field and its orientation respect to crystallographic axis. Consequently the time response of the detector depends not only from its operating conditions (bias voltage and temperature) but also from the special configuration (coaxial or planar) with which it has been built. From the above discussion we can conclude that the knowledge of the transport properties are not only necessary for predicting the timing characteristics of the detectors but also its performance as spectrometers.

The kind of characteristics which are relevant in the material depend upon the use of the spectrometer. In fact if resolution is the main task, the material should have properties which are different if an easy handling is required. Moreover the kind of radiation to detect, i.e., γ-rays or charged particles, requires also convenient physical properties of the material. However in order to give an idea, the minimum requires for a detector with 1 keV resolution are[1]:

Atomic number $Z \simeq 40$
Detector thickness $L \simeq 2$ mm
Energy gap $E_g \simeq 1$ eV
Trapping center $N_T \leqslant 5\ 10^{12}\ cm^{-3}$
Carrier mobility $\mu \gg 100\ cm^2V^{-1}sec^{-1}$
Donors, acceptors $|N_A - N_D| \leqslant 5\ 10^{11}\ cm^{-3}$
Contacts non injecting.

The aim of this work is to show the electron and hole transport properties in several semiconductor materials useful for making nuclear solid state detectors. Together classical semiconductor materials like silicon and germanium other materials like CdTe, GaAs and HgI_2 are also examined.

TRANSPORT PROPERTIES

In a solid state detector the collection of charge carriers created by a radiation

mainly occurs under the effect of an applied electric field. Such collection is mainly affected by the carrier drift velocity, which is the mean velocity that the carriers have under the effect of electric field. The carrier motion can be modified by capture and reemission on trapping centers whose presence in the material can strongly modify the pulse shape[1,14,16]. This pulse shape can also be modified by the plasma time[17,18,19] which mainly occurs with heavy ions like for instance alpha particles. We want also to point out that the thermal velocity of charge carriers is higher or at least comparable (depending upon the electric field and the operating temperature) with the drift velocity. Consequently the motion of the carriers due to the diffusion, may be, in some cases, not negligible[20]. In order to give a full picture of the motion of carriers in the semiconductor detector, we will now examine the transport properties which are relevant in solid state detectors.

a) Drift velocity.

The current density J due to the motion of charge carriers in a semiconductor material under the effect of an electric field E is $J = n\,q\,v_d$ where n is the carrier density moving with an average velocity v_d and q is the electronic charge. The drift velocity v_d is strongly affected by the electric field. In fact:

i) It is function of the electric field.

In fact at low electric field (e.g. E 2 KV/cm for electrons in Si at 300 K) the velocity is proportional to E (Ohmic region), at higher fields v_d increases slower than E and reaches a region (saturation region) where it is independent of E.

ii) It depends upon the orientation of the electric field respect to crystallographic axis of the material[21,22].

In some materials (e.g. electrons in CdTe and GaAs) the drift velocity increases with E until E reaches a certain value called threshold voltage (E_{th}) and above this value v_d decreases giving a negative differential mobility. Moreover the way in which drift velocity is affected by the electric field depends strongly upon the temperature.

b) Trapping.

The carriers, during their motion inside the semiconductor material, can be trapped by impurities in the crystal[1,14,16]. After spending some time in the center these trapped carriers can be re-emitted[1,14,16] into conduction (or valence) band. Such phenomena can be described by two time constants: the mean free drift time τ^+ and the detrapping time τ_D.

i) Mean free drift time τ^+.

If in the material trapping centers are present uniformely distributed and τ_D is infinite the numbers n of free carriers decreases with time[1,14,16] as

$$n = n_0 \exp(-t/\tau^+) = n_0 \exp(-x/\lambda)$$

where $x = v_d t$, n_0 is the total carrier created and λ is the mean free drift length of the carriers. Obviously only in the case where λ is much higher of the total thickness of the detector the signal shape is not appreciable modified.

ii) Detrapping time τ_D.

The carriers trapped can be reemitted in conduction or valence band and again contribute to the motion. If the re-emission is due to a thermal process the probability of such process is[1,14,16]

$$\frac{1}{\tau_D} = S \exp(-E_T/KT)$$

where S is a "frequency factor" and E_T is the level of the trapping center. Values of τ_D can be obtained from the analysis of the current and voltage waveforms induced at the contacts by the motion of the charge carriers.

When τ_D is much larger both τ^+, T_R and there is only one trapping center uniformely distributed for the kind of carrier considered than the mean free drift time can be measured in two ways[16,23]:

i) from the shape of the current pulse.

In fact:

$$I(t) = \frac{n_0 q}{T_R} \exp(-t/\tau^+) \quad \text{for } t \leq T_R$$

$$I(t) = 0 \quad \text{for } t > T_R$$

ii) from the amplitude of the voltage pulse V(t).

In fact from the Hetch formula[16,23]

$$V(t) = \frac{n_0 q}{C} \frac{\tau^+}{T_R} (1 - \exp(-t/\tau^+)) \text{ for } t \leq T_R$$

Knowing T_R and n_0 we can obtaine τ^+.

In general the analysis of the current pulse gives better results, but if τ^+ or T_R are less than 5 nsec the voltage pulse is preferable.

If the detrapping time is not negligible, the voltage pulse has a "fast" and a "slow" component. The fast component is given by:

$$V(t) = \frac{n_0 q}{C} \frac{\tau_e}{T_R} \left[\frac{t}{\tau_D} + \frac{\tau_e}{\tau^+} (1 - \exp(-t/\tau_e)) \right] \quad \text{for } t \leq T_R$$

$$\tau_e = \frac{\tau^+ \tau_D}{\tau^+ + \tau_D}$$

For the slow component ($t > T_R$) it is impossible to give an analytical relationship. However the time behaviour of V(t) in the case of "fast" and "slow" component can often[16] be characterized by a rise time t' defined as the

time when the voltage pulse reach 72% of its maximum value and is given by

$$t' = \frac{T_R}{\tau^+} \tau_D + T_R .$$

t' is the time (τ_D) that the carriers spent in the traps multiplied by the average number of trapping events (T_R/τ^+) plus the transit time T_R.

The electric field E can influence τ^+ essentially in two ways. One is a reduction of the potential barrier associated to the trapping center. This effect, called Poole-Frenkel effect, causes an increase of τ^+[16,24]. This mechanism is important only when the potential barrier is lowered by the field by a quantity of the order of at least KT. The second mechanism which causes a increase of τ^+ is the well known "heating" effect of the carriers by the electric field. According to the Lax theory[25] τ^+ should increases proportionally to $(T_L/T_e)^2$ where T_L is the lattice temperature and T_e is the carrier temperature assuming a maxwellian distribution function.

The detrapping time can be enhanced by the electric field in two ways depending upon the activation energy of the trap and the magnitude of the applied electric field. The first mechanism is the same Poole-Frenkel effect previously described which leads to a decrease of the trap potential barrier by a quantity proportional to $E^{1/2}$[25]. The second mechanism which generally occurs at electric field much higher than the other is the tunnel effect which leads to a temperature independent re-emission process[27,28,29].

c) Plasma time.

The electron and hole pairs generated by a strongly ionizing radiation such as alpha particles inside the detector have such a high density (of the order of 10^{19} cm^{-3}) that as soon as the opposite charge carriers begin to separate under the action of the electric field a counter electric field is generated. The drift of carriers is then substantially blocked until, owing to diffusion, the density falls to lower values, and carriers start to move[17,18,19]. However, the charge drifted is still slowed down by the influence on the electric field of the density of the charges to be collected[17,19]. Such phenomena beside giving a delay[18] of the pulse with respect to the arrival of the ionizing radiation, give an increase of the pulse rise time[17,19]. These effects generally decrease by increasing the electric field and strongly depend upon the kind of ionizing radiation.

DRIFT VELOCITY DATA

The major part of the experimental results reported in the following have been obtained with the time-of-flight technique which is the best technique to measure not only v_d but also the other quantities connected with the transport of charge carriers. The time-of-flight technique has been extensively described elsewhere[16,30] and here we restrict ourself by saying that such technique is based on the measurements of the time that electrons or holes created by a suitable ionizing radiation spend to cross under the effect of an applied electric field E, the known thickness W of a sample. With the time-of-flight technique not only it is possible to use the same type of materials used to make solid state detectors but also the working principles are the same as in these devices. Thus the velocity data obtained with this technique are the ones to be used in predicting the performance of solid state detectors. Other techniques, like for instance Hall effect, give mobility data which are not affected by trapping and detrapping effects[31]. Therefore they are less useful, expecially in the case of compensated materials, where such effects are present.

The theoretical interpretation[22] of the drift velocity data can be performed by tacking into account the band structure parameter and the interactions of the carriers with the lattice, with the impurities of the materials and among the carriers themselves. At the present the best way to solve the transport problem is to use a simulation Monte Carlo technique in which the motion of a single carrier is followed for a given length of time together with its collisions[30,32]. The reliability of such technique depends not only upon the precision with which the simulation is performed but also upon the knowledge of the band structure and the different scattering mechanisms which determine such motion.

Silicon

Silicon has been intensively studied since several years mainly because it is the most important material in semiconductor physics and solid state electronics. Many papers concerning the carrier transport properties have been published[33-37] but the most complete set of data concerning a large range of temperatures (6-430 K) and electric field (1-5 x 10^4 V/cm) applied parallel to ⟨111⟩ , ⟨100⟩ and ⟨110⟩ axis has been reported by the Modena group[38-40]. Their data, where a comparison is possible are in agreement with those of other authors. The measurements were performed with the time-of-flight technique in high purity silicon.

In Fig. 1, 2 and 3, the electron drift velocity is reported as a function of temperature and electric field as solid lines which represent the average value of the experimental data since the spread of the data obtained in different samples is very small (within few

percent). The electric field is applied parallel to ⟨111⟩ and ⟨100⟩ crystallographic axis in Fig. 1 and 2 respectively.

The mean features of the experimental results are:

i) At the highest electric field, particularly when E is applied parallel to the ⟨111⟩ axis, a region of drift velocity nearly independent of the electric field is obtained. Saturation drift velocity for electrons, which has been measured also by Rodriguez and Nicolet[41] between 4.2 and 300 K and by Duh and Moll[42] between 77 and 400 K, was found to be nearly independent of temperature between 4.2 and 77 K and to decrease by increasing the temperature.

ii) The anisotropy effect (see Fig. 3) that is the difference between the electron drift velocity with the electric field applied parallel to ⟨111⟩ (v_{111}) ⟨100⟩ (v_{100}) and ⟨110⟩ (v_{110}) crystallographic axis, is present at all examinated temperatures. The electron drift velocity v_{111} is larger than v_{100}. This anisotropic effect increases and start at lower electric field at decreasing temperatures. The curves of the drift velocities along the two directions ⟨111⟩ and ⟨100⟩ , tend to join together at a value of the electric field increasing with temperature, even though such a rejoning has not been experimentally reached at all considered temperatures.

iii) A negative differential mobility region (NDM) was found when the electric field is applied parallel to the ⟨100⟩ direction for temperatures below 40 K. This effect is enhanced by decreasing the temperature. The threshold field, defined as the field where the drift velocity has the maximum value before the region of negative differential mobility decreases at decreasing temperatures.

iv) For $T \geqslant 45$ K the Ohmic region is experimentally reached and the results are in good agreement with values for the mobility given in literature. For $T < 45$ K even at lowest applied field, the drift velocity is not proportional to the electric field indicating that Ohmic conditions are not reached. However at the lowest temperatures the data obtained with the time-of-flight technique are the highest ever measured.

Experimental results of hole drift velocity obtained in the same wide ranges of temperatures and electric fields applied parallel to ⟨100⟩ and ⟨110⟩ crystallographic directions, are shown in Fig. 4, 5, 6. The main features of the present results can be summarized as follows:

i) Even at the highest applied field saturation drift velocity was not reached in Si at any temperature.

ii) The holes drift velocity exhibit an anisotropic behaviour with v_{100} higher than v_{111} contrarly to the electron case. The anisotropy is best evidenced at the lowest temperature (see Fig. 6 a and b) where its maximum effect is of about 20%. Furthermore anisotropy appears to saturate at the highest fields, near about 10^4 V/cm, for $T \lesssim 77$ K.

iii) A well defined saturation region of v_d for the three different directions shows up in a narrow range of fields between 50 and 150 V/cm at 6 K. This effect smooths by increasing the temperature till being no more detectable by experiments for temperatures above about 40 K.

iv) The mobility obtained for the lowest value of the applied electric field exhibits a sudden increase for temperatures below about 30 K giving expectation of an anomalous behaviour of the lattice controlled ohmic mobility.

A quantitative analysis of these experimental data is difficult and away from the purpose of the present paper. However on the basis of the conduction and valence band structures of silicon a quantitative interpretation is possible[39]. The anisotropy effect and negative differential mobility of electrons is predominantly due to repopulation[39] of carriers in six equivalent valleys around the six minima of the conduction band along the main crystallographic direction ⟨100⟩ . If the electric field is not applied along a crystallographic direction which sees the valleys as equivalent, as for example the ⟨111⟩ direction in silicon, the different valleys contribute with different partial drift velocities and, different heating of the electrons in the different valleys (hot and cold) generates also a repopulation of the valleys themselves.

The anisotropy effect of holes is mainly due to the pronounced warping[40] exhibited by the heavy hole band which dominates the transport properties of hot holes. The anomalous behaviour in the temperature dependence of the hole ohmic mobility and the net defined saturation region of v_d found in a narrow range of fields at very low temperatures, may be ascribed[43] to the strong non parabolicity of the silicon valence band structure.

Germanium

Germanium is the semiconductor material most widely used in making solid state detectors. Its properties have been extensively studied and the results are reported in several papers[44-50]. Here we report the electron and hole drift velocities as functions of temperature and electric field applied parallel to ⟨111⟩ and ⟨100⟩ crystallographic directions. Most of the data have been obtained in high purity germanium with the time-of-flight technique[16]. These data are not affected by impurity scattering or by trapping detrapping effect.

In Fig. 7, 8, 9 the experimental drift velocity of electrons is reported with the electric field applied parallel to ⟨111⟩ and ⟨100⟩ crystallographic axis. A set of data are also obtained by Chang and Ruch[46] and Neukermans and Kino[44] with the time-of-flight technique. The main features of these results are:

i) The anisotropy (see Fig. 9), that is the difference in the drift velocity with electric field applied parallel to the two examinated axis, is present at all the considered temperatures. The drift velocity v_{111} is always larger than v_{100}. This effect increases by increasing the electric field or by decreasing the temperature. In the ohmic region, where v_d is proportional to E, the drift velocity is the same in both the directions.

ii) A negative differential mobility region appears at $T \leqslant 80$ K for electric field higher than 1 KV/cm applied parallel to ⟨100⟩ axis. This effect increases by decreasing the temperature.

In Fig. 10, 11, 12 the results obtained for holes are shown at different temperatures and for electric field applied parallel to the ⟨111⟩ and ⟨100⟩ crystallographic axes. The hole drift velocity in Ge, contrarly at what happens in silicon, shows a continuous increase with electric field up to the saturation. The values of drift velocity indicate that saturation is obtained for field strenghs greater than about 5 10^3 V/cm at temperatures below 100 K. These limiting values range from 1.1 10^7 cm/sec at 100 K to 1.3 10^7 cm/sec at 8 K for E // ⟨100⟩ and 9 10^6 cm/sec at 80 K to 9.5 10^6 cm/sec at 40 K for E // ⟨111⟩. The anisotropic effect is clearly evidenced in Fig. 12 and increases by decreasing the temperature.

Like in the case of silicon, the anisotropy in the hole drift velocity is due to the warped shape of germanium valence band[51]. The negative differential mobility found for electrons is due to the transfer of electrons from the ⟨111⟩ minima to the higher ⟨100⟩ minima. The separation of these two minima is 0.21 eV and the ratio of the effective masses makes the situation similar to the intervalley transfer mechanism leading to NDM in GaAs or CdTe.

A second region of NDM at electric field lower than 10 V cm^{-1} applied parallel to ⟨111⟩ axis for temperatures below 30 K was also found[52]. The effect is due, like in silicon, to the heating of electrons and to the consequent transitions of these electrons from valleys which have a lower value of the effective mass in the direction of the applied field to valley which have in the same direction an higher value of the effective mass.

Cadmium Telluride

Cadmium telluride is the most promising semiconducting material for making γ-ray detectors working at room temperature[53]. Altough the device performance at present is inadeguate because of poor charge transport, due to the quality of the material, it is improving. The limitation is mainly due to the low $\mu\tau^+$ value for hole. The measurements reported[54,55] here have been performed in high resistivity material, Cl or In doped, with the time-of-flight technique. While the results for electrons approaches, expecially at high field (f.i. at 300 K, E 2 KV/cm) the pure lattice drift velocity the data for holes show clearly a strong dependence of trapping detrapping effect[55]. An overall picture of the measured electron drift velocities as a function of electric field and for temperatures ranging from 77 to 370 K is shown in Fig. 13 where a smooth curve was drawn through the data points. These curves clearly show a NDM and a peak velocity increasing from 1.25 10^7 cm/sec at 370 K to 2.5 10^7 cm/sec at 77 K. The value of the electric field E_{th} corresponding to the maximum drift velocity decreases from 16 KV/cm at 370 K to 11 KV/cm at 77 K.

The NDM is due to intervalley transitions between the central valley and secondary minima[56]. The threshold field E_{th} decrease with decreasing temperature because the contribution of the polar optical phonons to the total scattering process decreases with temperature and the instability situation, corresponding to a dramatic increase of electron energy is reached at lower electric field. For electric fields equal to or larger than E_{th} the mobility is determined by both intervalley and polar optical mode scattering. This explains the increase of both the maximum value of the drift velocity and the slope of the drift velocity in NDM region with decreasing temperature. For applied electric field below E_{th} and for temperatures lower than 370 K drift velocity increases faster than a linear relation with E (super-Ohmic behaviour). This effect seems due to a combined effect of polar optical phonon scattering and ionized impurities scattering[56]. The latter is predominant at lower temperatures. Further evidence of the ionized impurity effect is shown in Fig. 14 where the theoretical mobility[57] is compared, as a function of the temperature, with the experimental data obtained by the ratio v_d/E evaluated at 2 KV/cm.

The hole mobility is strongly affected by trapping and detrapping effect[55]. A typical set of data obtained in high resistivity material is shown in Fig. 15 as a function of temperature and electric field. These data, which represent the situation up to date,

show:
a) at a fixed electric field the mobility decreases with decreasing temperature,
b) at a fixed temperature the mobility increase with increasing electric field.
These behaviour, which is not due to the pure lattice scattering, is interpreted as due to trapping and detrapping effect and by the influence on these effects of the electric field throught the Poole-Frenkel mechanism. The continuous lines in Fig. 15 are the theoretical results assuming 5 10^{-16} cm^{-3} trapping centers with a level of 140 meV[55]. The temperature dependence of the mobility measured at the lowest applied electric field is reported in Fig. 16 compared with other experimental data and theoretical expectation considering only lattice scattering mechanism. Only around room temperature the data from high resistivity material approach the theoretical limit indicating that a considerable number of ionized impurities acting both as traps and as coulombic scattering center are present.

Gallium Arsenide

Of all semiconductor compounds GaAs has received the most attention[30], primarily due to its numerous device applications. While the earlier boat grown material exhibited a too high trap density to be useful as radiation detector, the much purer epitaxial material available today has demonstrated its ability to provide spectrometer performance. The transport properties of the electrons in GaAs reported here in Fig. 17 have been investigated with the time-of-flight technique by J.G. Ruch and G.S. Kino[59]. The data show a linear increase of drift velocity at increasing electric field up to the threshold field 3 ÷ 3.5 KV/cm and above this value the drift velocity decrease. The large spread of the experimental data[30] obtained with many different techniques and in high or low resistivity material may be attributed to the amount of impurities present in the material. Let us remember that the negative differential mobility in GaAs is due to the band structure of this material characterized by a low-mass, high mobility valley, lying lower in energy than other high-mass, low mobility valley[32]. The energy separation of these two valleys lower in GaAs than in CdTe, justifies the smaller threshold field in GaAs.

In spite of its large importance very few measurements of hole mobility as a function of electric field and temperature are reported in literature. The drift velocity field curve for holes in p-GaAs has been experimentally determined, with ac conductivity technique at 300 K on ⟨111⟩ oriented samples, by V.L. Dalal[60], and is reported in Fig. 18. The drift velocity becomes a sublinear function of field around E = 1.5 10^4 V/cm, but no saturation was observed up to 6 10^4 V/cm.

Mercury Iodide

The use of HgI_2 as a radiation detector was introduced by Willing and Roth[61]. Very recently several measurements[62-65] of carrier drift velocity in HgI_2 have been performed with the time of flight technique. The examinated material was grown by vapour phase transport under a controlled thermal gradient. From crystals several cm^3 in size, samples have been cleaved with a thickness ranging from 40 to 500 μm. The main source of error in determining the drift velocity of charge carriers is due to the difficulties to measure the thickness of the cleaved sample.

In Fig. 19 and 20 are plotted the dependence of the mobility on the temperature for electrons and holes respectively. The results can be summarized as follows. The drift velocity of electrons is proportional to the electric field between 1.8 KV/cm and 40 KV/cm in the full examinated temperature range (80-350 K). The mobility increases with decreasing temperature following a power law $T^{-0.9}$. Its value at room temperature is equal to 100 cm^2 $V^{-1}sec^{-1}$.

Recently Martin et al.[62] have found for electrons a negative differential mobility for electric field higher than 80 KV/cm.

The mean free drift time of the holes in the examinated material was as low as few nsec. For this reason we could perform only measurements using very high electric fields at which the transit time T_r is less than the free drift time. The dependence of the hole mobility upon the temperature shows two different regions; a slope $T^{-1.75}$ between 140 and 240 K and a slope $T^{-3.5}$ between 240 and 350 K has been found. At room temperature the hole mobility is 4 cm^2 V^{-1} sec^{-1}.

CONCLUSIONS

The charge carrier transport properties of semiconductor materials suitable for making γ-ray detectors have been revised. Together with classical materials like silicon and germanium, other materials like CdTe, GaAs and HgI_2 have also been analyzed.

Materials like silicon and germanium are available at so high purity level that charge carriers transport properties are not affected by impurities down to about 20 K. As general behaviour the drift velocity increases by decreasing the temperature or increasing the electric field. However the variation is

stronger at low electric field and at high temperature. The anisotropic effect is investigated both in silicon and germanium. For the case of germanium the percentage variation of the drift velocity with electric field applied parallel to ⟨111⟩ and ⟨100⟩ axis is 25% for electrons and 20% for holes at 77 K. In all the case $v_{111} < v_{100}$.

Cadmium telluride, the most promising semiconductor material for γ-ray detectors working at room temperature, exhibits transport properties which are affected by scattering with impurities for electrons and by trapping and detrapping effects for holes. These effects, negligible at room temperature, depend strongly by the electric field and temperature. We must also point out that while the timing properties are controlled by the shallow levels (20 meV for electrons and 140 meV for holes) the resolution power (FWHM) is determined by deeper levels (50 meV for electrons and 400 meV for holes). The level at 400 meV seems the one responsible for the low $\mu\tau^{+}$ product for holes which limits at present the performance of the spectrometer.

The electron transport properties in GaAs are controlled below the threshold field by impurities even at room temperature. Very little is known about transport properties of holes and the only available measurements were obtained in low resistivity material at room temperature. A big effort should be made before GaAs becomes competitive with CdTe.

Mercury iodide is the most recent material available for making γ-ray detectors. Its transport properties seem controlled by lattice scattering and no effect of impurities have been detected. However the low values of mobilities (100 $cm^2\ V^{-1}\ sec^{-1}$ for electrons and 4 $cm^2\ V^{-1}\ sec^{-1}$ for holes at room temperature) limits strongly its application field.

ACKNOWLEDGEMENTS

We like to thank M. Martini for the useful suggestions and R. Minder, G. Majni and C. Jacoboni for the many helpfull discussions.

REFERENCES

1. G. Bertolini and A. Coche editors, "Semiconductor radiation Detectors" (North-Holland, Amsterdam, 1968).
2. W. Shockley, Cech. J. Phys., B11 (1968) 81.
3. C.A. Klein, J. Appl. Phys., 39 (1968) 2029.
4. E. Antoncik, G. Cola and L. Farese, Rad. Effects, 5 (1970) 1.
5. W.E. Drummond and J.L. Moll, J. Appl. Phys., 42 (1971) 5556.
6. C. Bussolati, A. Fiorentini and G. Fabri, Phys. Rev., 136 A (1964) 1756.
7. F.E. Emery and T.A. Rabson, Phys. Rev., 140 A (1965) 2089.
8. W.R. Dodge, S.R. Domen, T.F. Leedy and D.M. Skopik, Phys. Rev. Letters, 17 (1966) 658.
9. J.R. Key and T.A. Rabson, IEEE Trans. Nucl. Sci., NS-18, n° 1 (1971) 184.
10. C. Canali, M. Martini, G. Ottaviani and A. Alberigi Quaranta, IEEE Trans. Nucl. Sci., NS-19, n° 4 (1972) 9.
11. R. Ryan, IEEE Trans. Nucl. Sci., NS-20, n° 1 (1973) 473.
12. R.H. Pehl, F.S. Goulding, D.A. Landis and M. Lenzlinger, Nucl. Instr. and Meth., 59 (1968) 45.
13. A. Alberigi Quaranta, C. Canali, G. Ottaviani and K. Zanio, Lettere Nuovo Cimento, 4 (1970) 908.
14. M. Martini and T.A. McMath, Nucl. Instr. and Meth., 79 (1970) 259.
15. K.R. Zanio, W. Akutagawa and J.W. Mayer, Appl. Phys. Letters, 11 (1967) 5.
16. M. Martini, J.W. Mayer and K.R. Zanio, in: Applied Solid State Science, Ed. R. Wolfe, Academic Press, New York 1972, Vol. 3.
17. A. Taroni and G. Zanarini, Nucl. Instr. and Meth., 67 (1969) 277.
18. A. Alberigi Quaranta, A. Taroni and G. Zanarini, Nucl. Instr. and Meth., 72 (1969) 72.
19. P.A. Tove and W. Seibt, Nucl. Instr. and Meth., 51 (1967) 261.
20. J.W. Caywood, C.A. Mead and J.W. Mayer, Nucl. Instr. and Meth., 79 (1970) 329.
21. E.G.S. Paige, in: Progress in Semiconductors, Eds. A.F. Gibson and R.E. Burgess, Heywood Book, London 1964, Vol. 8.
22. E.M. Conwell, in: Solid State Physics, Eds. F. Seitz and D. Turnbull, Suppl. 9, Academic Press, New York (1967).

23. C. Canali, M. Martini, G. Ottaviani, A. Alberigi Quaranta and K.R. Zanio, Nucl. Instr. and Meth., 96 (1971) 561.

24. G.A. Dussel and K.W. Böer, Phys. Status Solidi, 39 (1970) 197.

25. M. Lax, Phys. Rev., 119 (1960) 1502.

26. J.L. Hartke, J. Appl. Phys., 39 (1968) 4871.

27. R.R. Hearing, Can. J. Phys., 37 (1959) 1374.

28. M. Martini and T.A. McMath, Nucl. Instr. and Meth., 79 (1969) 259.

29. C. Canali, F. Nava, G. Ottaviani and K.R. Zanio, Solid State Commun., 13 (1973) 1255.

30. A. Alberigi Quaranta, C. Jacoboni and G. Ottaviani, Rivista Nuovo Cimento, 1 (1971) 446.

31. E.H. Putley, "The Hall Effect and Semiconductor Physics". Dover Publications, Inc. New York, 1968.

32. W. Fawcett, A.D. Boardman and S. Swain, J. Phys. Chem. Solids, 12 (1970) 1963.

33. A.C. Prior, J. Phys. Chem. Solids, 12 (1959) 175.

34. T.E. Seidel and D.L. Scharfetter, J. Phys. Chem. Solids, 28 (1967) 2563.

35. C. Norris and J.F. Gibbons, IEEE Trans. on Electron Devices, ED-14 (1967) 38.

36. M. Costato and L. Reggiani, Phys. Rev., 3B (1971) 1501.

37. P.A. Tove, G. Andersson, G. Ericsson and R. Lidholt, IEEE Trans. on Electron Devices, ED-17 (1970) 407.

38. C. Canali, G. Ottaviani and A. Alberigi Quaranta, J. Phys. Chem. Solids, 32 (1971) 1707.

39. C. Canali, C. Jacoboni, F. Nava, G. Ottaviani and A. Alberigi Quaranta, submitted to Phys. Rev.

40. G. Ottaviani, L. Reggiani, C. Canali, F. Nava and A. Alberigi Quaranta, submitted to Phys. Rev.

41. V. Rodriguez and M.A. Nicolet, J. Appl. Phys., 40 (1969) 496.

42. C.Y. Duh and J.L. Moll, IEEE Trans. Electron Devices, ED-14 (1967) 46.

43. C. Canali, M. Costato, G. Ottaviani and L. Reggiani, Phys. Rev. Letters, 31 (1973) 536.

44. A. Neukermans and G.S. Kino, Phys. Rev., 7B (1973) 2693.

45. M.I. Nathan, Phys. Rev., 130 (1963) 2201.

46. D.M. Chang and J.G. Ruch, Appl. Phys. Letters, 12 (1968) 111.

47. E. Sakai, H.L. Malm and I.L. Fowler, Proceedings of Gatlinburg Conference, Publication 1593, National Academy of Science, Washington D.C. (1969) p. 101.

48. W. Sasaki and M. Shibuya, J. Phys. Soc. Japan, 11 (1956) 1202.

49. G. Ottaviani, C. Canali, F. Nava and J.W. Mayer, J. Appl. Phys., 44 (1973) 2917.

50. C. Canali, G. Ottaviani and G. Majni, Solid State Commun., 15 (1974) 1213.

51. L. Reggiani, C. Canali, F. Nava and G. Ottaviani, Proceedings of 12 International Conference on the Physics of Semiconductors, July 15-19, 1974 Stuttgart, p. 819.

52. A.A. Kastalskii and S.M. Ryvkin, Proceedings of IX Conference on the Physics of Semiconductors, July 23-29, 1968 Moscow, p. 955.

53. See the Proceedings of the "International Symposium on Cadmium Telluride" June 29-30, 1971 Strasbourg.

54. C. Canali, M. Martini, G. Ottaviani and K.R. Zanio, Phys. Rev., 4B (1971) 422.

55. G. Ottaviani, C. Canali, C. Jacoboni, A. Alberigi Quaranta and K.R. Zanio, J. Appl. Phys., 44 (1973) 360.

56. V. Borsari and C. Jacoboni, Phys. Stat. Solidi (b), 54 (1972) 649.

57. B. Segall, M.R. Lorenz and R.E. Halsted, Phys. Rev., 129 (1963) 2471.

58. M. Aven and J.S. Prener, Physics and Chemistry of II-VI Compounds (North-Holland, Amsterdam, 1967).

59. J.G. Ruch and G.S. Kino, Phys. Rev., 174 (1968) 921.

60. V.L. Dalal, Appl. Phys. Letters, 16 (1970) 489.

61. S. Roth and W.R. Willig, Appl. Phys. Letters, 18 (1971) 328.

62. G.M. Martin, P. Boch and P. Guétin, Appl. Phys. Letters, 25 (1974) 286.

63. R. Minder, G. Majni, C. Canali, G. Ottaviani, R. Stuck, J.P. Ponpon, C. Schwab and P. Siffert to be published on J. Appl. Phys.

64. H.L. Malm, IEEE Trans. on Nucl. Sci., NS-19 (1972) 263.

65. J. Llacer, M. Watt, M. Schieber, M. Carlston and W. Schnepple, IEEE Trans. on Nucl. Sci., NS-21 (1974) 302.

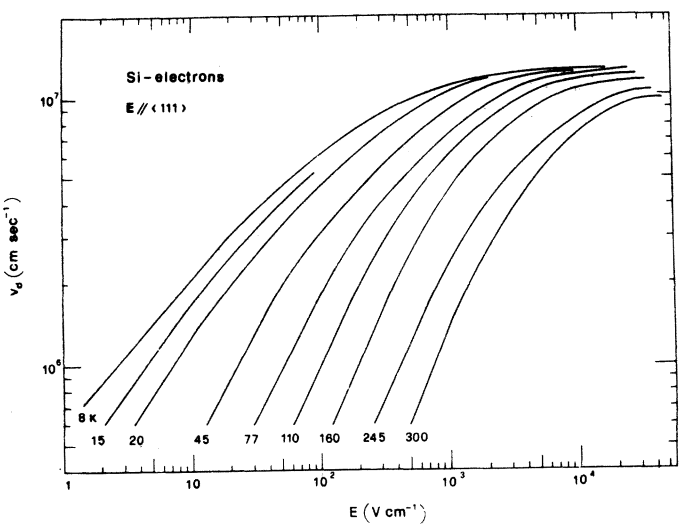

Fig. 1 - Experimental electron drift velocity in silicon as a function of electric field applied parallel to ⟨111⟩ direction at different temperatures.

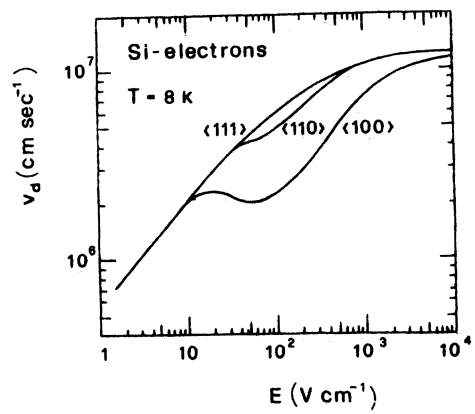

Fig. 3 - Experimental electron drift velocity in silicon as a function of electric field at T = 8 K with the field applied parallel to ⟨111⟩, ⟨100⟩ and ⟨110⟩ directions as indicated to the figures.

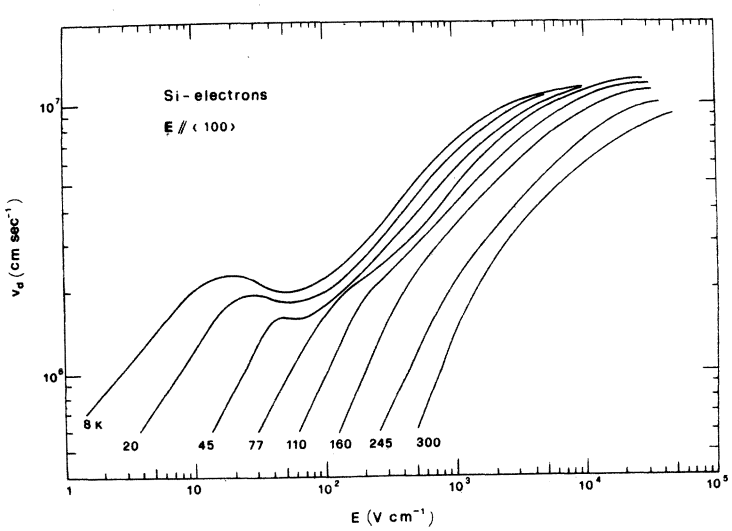

Fig. 2 - Experimental electron drift velocity in silicon as a function of electric field applied parallel to ⟨100⟩ direction at different temperatures.

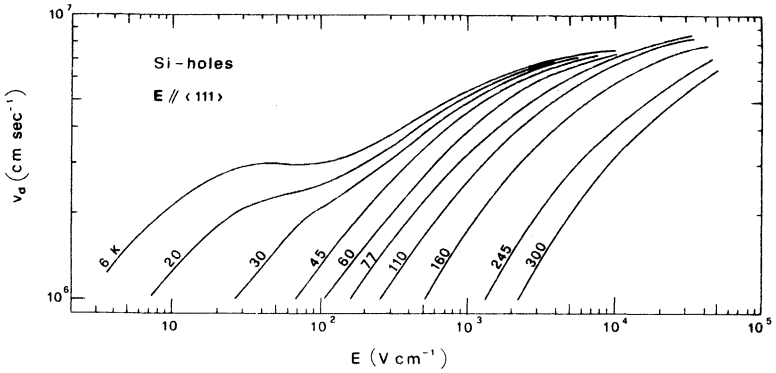

Fig. 4 - Experimental hole drift velocity in silicon as a function of the electric field applied parallel to ⟨111⟩ crystallographic axis at different temperatures.

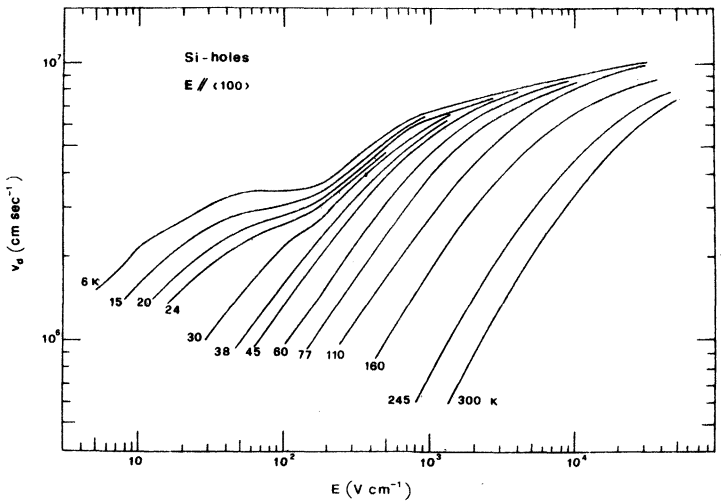

Fig. 5 - Experimental hole drift velocity in silicon as a function of electric field applied parallel to ⟨100⟩ axis at different temperatures.

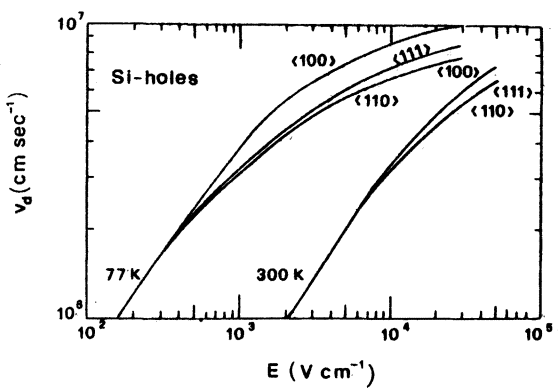

Fig. 6 - Hole drift velocity in silicon as a function of electric field applied parallel to ⟨111⟩ , ⟨100⟩ and ⟨110⟩ axis at 77 and 300 K.

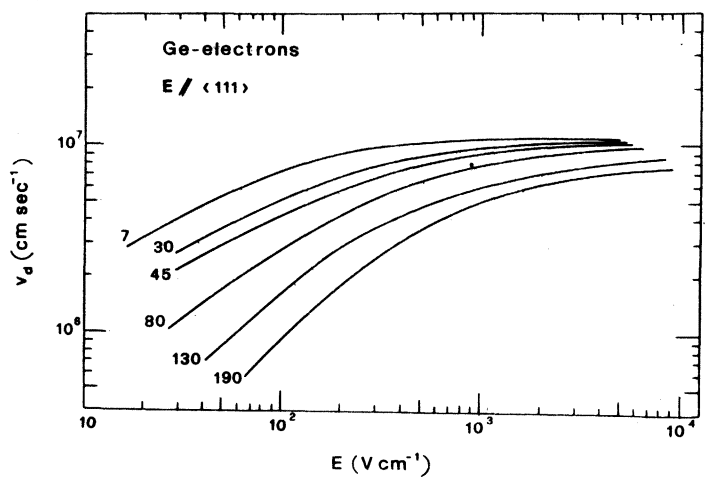

Fig. 7 - Experimental electron drift velocity in germanium as a function of electric field applied parallel to ⟨111⟩ direction at different temperatures.

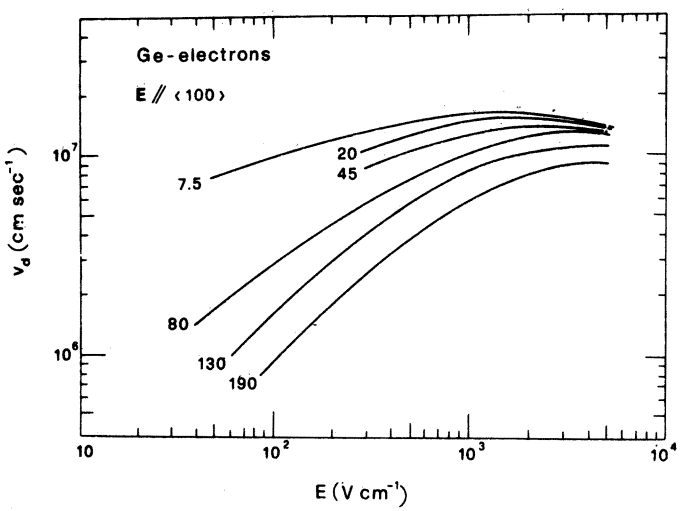

Fig. 8 - Experimental electron drift velocity in germanium as a function of electric field applied parallel to ⟨100⟩ direction at different temperatures.

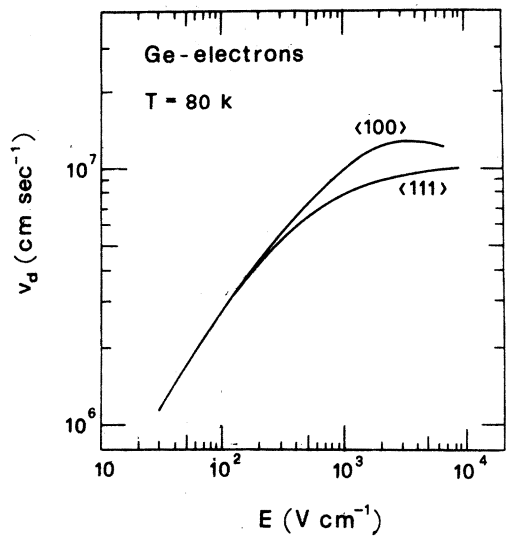

Fig. 9 - Electrons drift velocity in germanium with electric field applied parallel to ⟨111⟩ and ⟨100⟩ axis at 80 K.

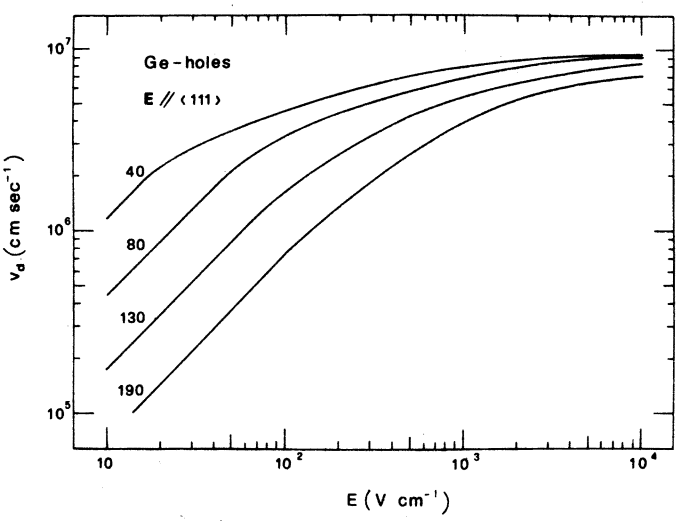

Fig. 10 - Experimental hole drift velocity in germanium as a function of the electric field applied parallel to ⟨111⟩ crystallographic axis at different temperatures.

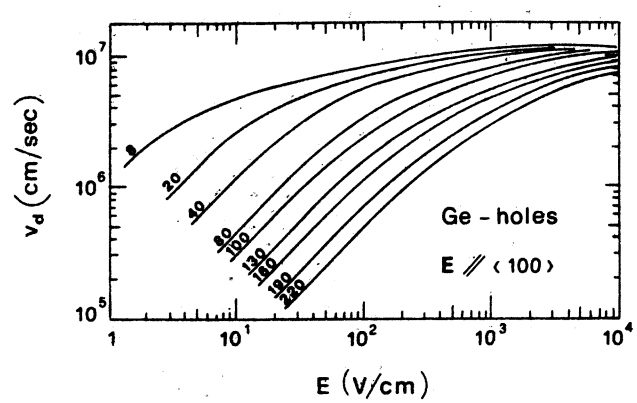

Fig. 11 - Experimental hole drift velocity in germanium as a function of electric field applied parallel to ⟨100⟩ axis at different temperatures.

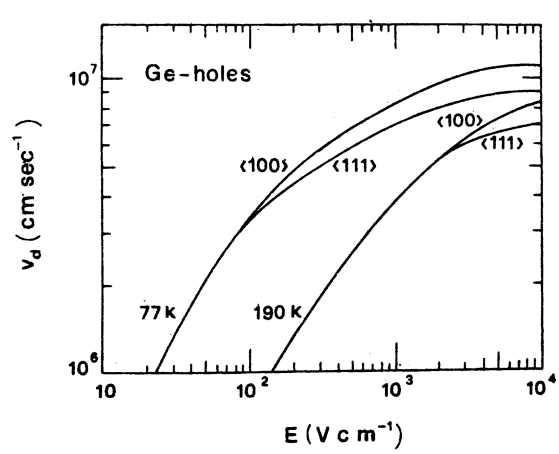

Fig. 12 - Holes drift velocity in germanium with electric field applied parallel to ⟨111⟩ and ⟨100⟩ crystallographic axis at 77 and 190 K.

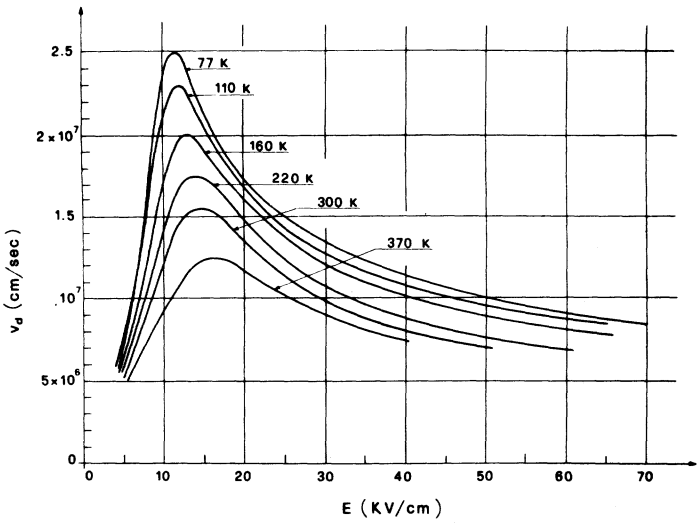

Fig. 13 - Electron drift velocity in CdTe as a function of electric field at different temperatures.

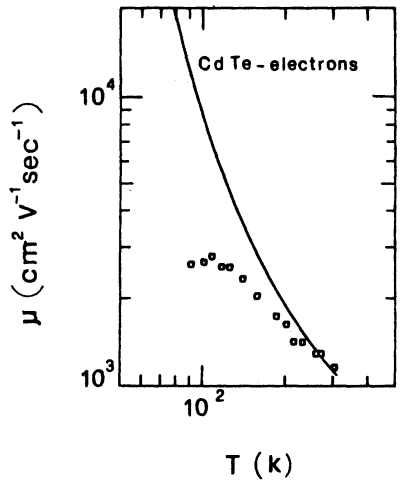

Fig. 14 - Electron drift mobility in CdTe as a function of temperature evaluated at 2 KV/cm. The continuous lines are theoretical data without impurities by Segall et al.[57] in agreement with experimental data obtained in low resistivity material and using Hall effect.

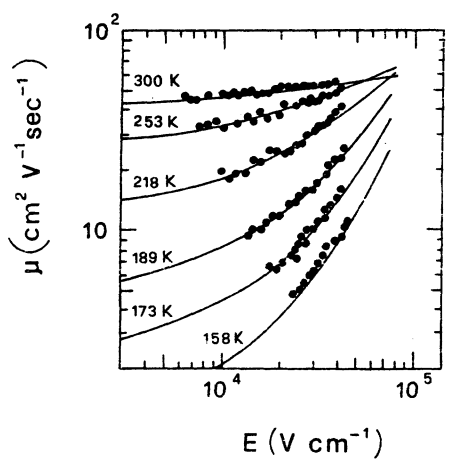

Fig. 15 - Hole mobility in CdTe as a function of electric field at different temperatures. Full lines show the theoretical results taking into account Poole-Frenkel effect.

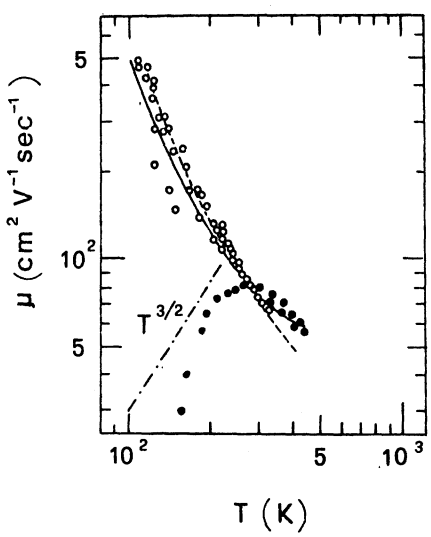

Fig. 16 - Hole mobility in CdTe as a function of temperature. Closed circle refers to our experimental data, open circles are from Yamada[58]. The solid line is the theoretical drift mobility obtained with the Monte Carlo calculations[56] while the dashed line came from[58] $\mu=57\ (\exp(252/T)-1)$.

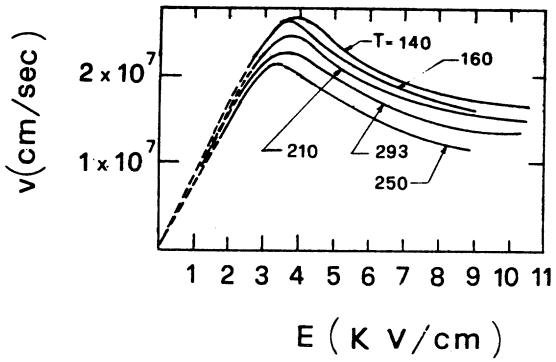

Fig. 17 - Electrons drift velocity in GaAs as a function of electric field at five different temperatures obtained by Ruch and Kino[59].

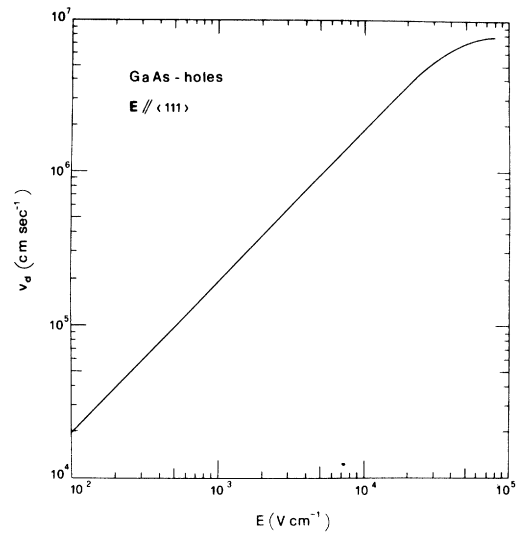

Fig. 18 - Hole drift velocity in GaAs as a function of electric field at room temperature obtained by Dalal[60].

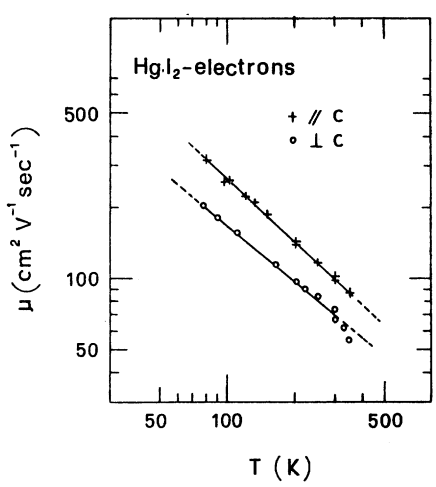

Fig. 19 - Electrons mobility in HgI_2 as a function of temperature. The electric field was applied parallel and perpendicular to C axis.

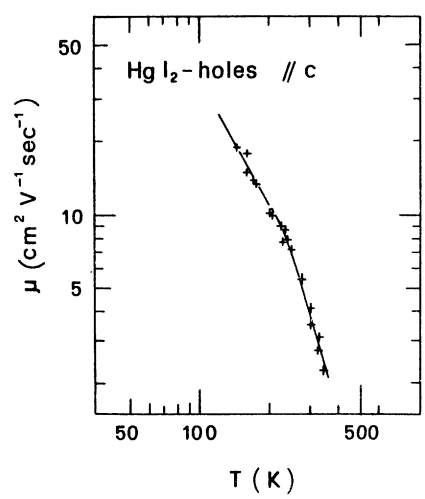

Fig. 20 - Hole mobility in HgI_2 at different temperatures.